

Comparative Transcriptional Analysis of Mouse Hybridoma and Recombinant Chinese Hamster Ovary Cells Undergoing Butyrate Treatment

Marcela De Leon Gatti,¹ Katie F. Wlaschin,¹ Peter Morin Nissom,²
Miranda Yap,² and Wei-Shou Hu^{1*}

Department of Chemical Engineering and Materials Science, University of Minnesota, 421 Washington Ave SE., Minneapolis, MN 55455-0132, USA¹ and Bioprocessing Technology Institute/A-STAR, 20 Biopolis Way #06-01 Centros, Singapore 138668, Singapore²

Received 5 June 2006/Accepted 24 October 2006

DNA microarray based transcriptome analysis has become widely used in biomedical research; however, the lack of DNA sequence information available for Chinese hamster ovary (CHO) cells has hampered the application of microarrays for this cell line widely used for recombinant therapeutic protein production. We have constructed an expressed sequence tag (EST) based CHO DNA microarray and employed it for comparative transcriptome analysis of CHO cells and mouse hybridoma cells treated with sodium butyrate. Cross-species hybridization of CHO transcripts to mouse DNA microarrays was also performed to assess the utility of cross-species microarray. The average identity among probe sequences present on both the CHO and mouse microarray was 89.6%. Although cross-species hybridization yielded non-contradicting results when compared with the same-species arrays, decreased sensitivity was observed and resulted in fewer differentially expressed genes being confidently identified. The comparatively small number of genes probed using the CHO microarray and the low number of genes identified as differentially expressed in the cross-species hybridization limited physiological interpretation of the response of CHO cells to sodium butyrate treatment. Nevertheless, when all results are combined, mouse hybridoma and CHO cells can be seen to respond similarly to butyrate treatment, affecting histone modification, chaperones, lipid metabolism, and protein processing. To further develop the utility of microarray technology in cell culture process development, an expansion of current CHO cell sequencing efforts to increase the coverage of genes on available microarrays is warranted.

[Key words: cell culture, genomics, transcriptome, cross-species hybridization, expressed sequence tag (EST), butyric acid, cDNA microarray, antibody production]

Over the past two decades, mammalian cell culture has evolved to become the most important bioprocess for production of recombinant protein therapeutics. The vast majority of the recombinant mammalian cell products are produced in rodent derived cells; primarily, mouse myeloma cells, and Chinese hamster ovary (CHO) cells. Along with the development of mammalian cell based bioprocessing, much work has been done to optimize culture productivity, primarily through media design and control of environmental conditions. Increasingly, metabolic engineering is being employed as a means to confer cells with characteristics desired in bioprocessing, including altered metabolic properties, improved resistance to stress-induced cell death, and improved product quality (1).

The increasing availability of genomic information, in the form of both complete genome sequence assemblies and expressed sequence tags (ESTs), offer greater opportunity for

cell line development and bioprocess optimization. High-throughput comparative expression monitoring tools hold the potential to identify genes playing critical roles in rendering cells or processes with better characteristics. Metabolically engineering cells through those may lead to cell lines harboring superior production characteristics.

One of the most complex, yet highly desired traits of recombinant protein producing cell lines is a high specific productivity; yet, little is understood about the cellular characteristics associated with hyperproductivity. A hyperproducing cell line is expected to have a high protein secretion and processing capacity, with sufficient energy generation machinery. A survey of transcriptomes of hyper-producing cells and culture conditions known to increase productivity could lead to the identification of genes and other molecular markers playing key roles in productivity. Unfortunately, among the rodent species whose cells are used widely in bioprocessing, *Mus musculus* is the only one with extensive genomic resources, including a completed genome sequence assembly, a large collection of functionally annotated ESTs,

* Corresponding author. e-mail: acre@cems.umn.edu
phone: +1-612-626-7630 fax: +1-612-626-7246

and commercially available microarrays. Although the cost of sequencing has reduced drastically in the last few years, the construction of libraries for EST sequencing and microarray fabrication is still a venture requiring considerable resources. An alternative to the construction of new DNA microarrays is to employ microarrays designed for another closely related species for cross-species hybridization. For CHO cells, we recently reported the construction of CHO cell cDNA libraries for EST sequencing and printing of a DNA microarray. The microarray contained 2602 unique sequences and was used to assess the utility of such resources for transcriptome surveys in CHO cell lines.

In this report, we compared transcript profiles of CHO cells and mouse hybridoma cells treated with sodium butyrate. Sodium butyrate is a histone deacetylation inhibitor, and has long been used to increase specific productivity of secreted proteins in hybridoma cells and other recombinant mammalian cells, including CHO cells (2–5). Examination of transcriptome profiles in both CHO and mouse cells, for which a much larger repertoire of well annotated genes are available on DNA microarrays, allows us to corroborate the results of transcriptome analysis with physiological knowledge. Hybridization of CHO cell mRNA to both mouse and CHO microarrays additionally provides a direct assessment of the suitability of using mouse probes for quantifying CHO cell transcriptome profiles and the need to further develop CHO cell line specific genomic resources.

MATERIALS AND METHODS

Cells and cell culture conditions The CHO and hybridoma (MAK) cell lines used in this study have been described previously (6, 7). The hybridoma cells were grown in DMEM:F12 (1:1) medium supplemented with 63.7 nM transferrin, 23.7 μ M 2-mercaptoethanol, 1.7 mM ethanolamine, 0.11 mM *l*-ascorbic acid, 28.9 nM sodium selenite and 6.2 μ M putrescine. The recombinant CHO cells were grown in the same media, and were additionally supplemented with 0.15 μ M methotrexate (MTX) and 0.01% (v/v) Intralipid emulsion (Sigma-Aldrich, St. Louis, MO, USA). Cells were grown in 100 ml spinner cultures to the mid-exponential stage, and were transferred into T-flasks prior to butyrate treatment. Cells were kept in a 37°C, 5% CO₂ environment. Cell concentration and viability were evaluated by manual counts on a hemocytometer after trypan blue staining.

Cell protein productivity determination Immunoglobulin G (IgG) concentration was measured by HPLC using a Protein G affinity column (Applied Biosystems, Foster City, CA, USA). Each sample (500 μ l) was loaded into a column. The buffers consist of 35 mM NaH₂PO₄, 15 mM Na₂HPO₄, 0.15 M NaCl (pH 7.0) for loading, and 0.15 M NaCl, 0.1% (v/v) HCl (pH 2.5) for elution. IgG detection was accomplished through UV absorbance at 280 nm (Beckman 166 Programmable Detector), and quantified through a calibration curve using serial dilutions of purified mouse IgG (Sigma-Aldrich).

Microarrays

cDNA microarrays The construction of the CHO cDNA libraries and microarray has been previously described (7). The array contained 4608 spotted cDNA probes representing 2602 unique transcripts. The mouse DNA microarray (BMAP) was also described previously (8), and contains 11568 sequences with 6608 unique transcripts. Annotation updates for sequences present in the mouse microarray were performed through the SOURCE program, available on the worldwide web (<http://genome-www5.stanford.edu/>

[cgi-bin/source/sourceBatchSearch](#)). Annotation of the CHO microarray sequences was previously described (7).

Orthologous genes represented in the CHO and mouse microarrays were identified through the BLAST (Basic Local Alignment Search Tool) program. All sequences present in the CHO array were compared to all the sequences present on the mouse array. An identity score and e-value were assigned to each sequence alignment and used to identify orthologous genes.

Sample preparation Cell samples were withdrawn from replicate hybridoma and recombinant CHO cultures at 0, 2, 4, 8, and 27 h after sodium butyrate addition. After sampling, the cell suspensions were centrifuged at 700 rpm for 5 min, and the cell pellet was flash frozen and stored in liquid nitrogen until RNA extraction. Total RNA was extracted with TriZol reagent (Invitrogen, Carlsbad, CA, USA) according to the manufacturer's protocol.

Four microarrays were hybridized for each time point using a duplicate dye-swap experimental design. For each array, 40 μ g of total RNA from each sample was used for first strand cDNA synthesis by reverse transcription using Superscript II Reverse Transcriptase (Invitrogen) in the presence of amino allyl-dUTP (Sigma-Aldrich) according to the manufacturer's protocol. The reaction was stopped by addition of 10 μ l of 1.0 N NaOH and 10 μ l 0.5 M EDTA and incubation at 65°C for 15 min, followed by neutralization with 25 μ l of 1.0 M Tris-HCl (pH 7.4). The amino-labeled cDNA was then purified using Microcon YM-30 filters according to the manufacturer's protocol (Millipore, Billerica, MA, USA). The sample was dried and resuspended in 9 μ l sodium bicarbonate buffer (pH 9.0) for 10–15 min at room temperature.

The entire recovered volume was transferred into dried Cy3 or Cy5-dye aliquots (Amersham Biosciences, Piscataway, NJ, USA) and incubated in the dark for 1 h. To prevent cross coupling between probes, 4.5 μ l of 4.0 M hydroxylamine was added and incubated for 15 min at room temperature in the dark. Labeled probes were purified using QiaQuick PCR purification columns, as per the manufacturer's instructions (Qiagen, Valencia, CA, USA). The hybridization probes were mixed with 25 μ l 2 \times hybridization buffer (50% formamide, 10 \times SSC and 0.2% SDS), 25 μ g mouse Cot-1 DNA, 20 μ g PolyA, 2 ng control genes and water to a final volume of 50 μ l.

Hybridization and array scanning Labeled hybridization probes were applied to the microarrays under lifter slips and incubated at 42°C for 12–16 h 3 \times SSC (10 μ l) was added to the chambers to prevent dehydration. The microarrays were removed from the hybridization chambers, submerged repeatedly for 1 min in 0.57 \times SSC and 0.02% SDS, transferred into 0.04 \times SSC and, again, submerged repeatedly for 1 min. Arrays were dried by centrifugation at 600 rpm for 5 min and stored in darkness until scanning. Images were obtained with the ScanArray 5000 microarray scanner (Express Packard BioScience Company, Meriden, CT, USA).

Data analysis and visualization Intensity data were extracted using GenePix Pro 4.1 analysis software (Axon Instruments, Union City, CA, USA). The data normalization was carried out with GeneSpring (Silicon Genetics, Redwood City, CA, USA) and median intensity values were normalized for each spot using the Loess method (9). Each spot was present in duplicate on both the CHO and BMAP microarrays. With four replicate microarrays hybridized at each time point, eight replicate data points were available for each probe. Statistical significance was assessed (*p*-values) using the Student's *t*-test to test the null hypothesis that the expression is unchanged between the two samples. The transcripts with a *p*-value lower than 0.05 and fold ratio higher than 1.4 in at least one of the four time points were identified as differentially expressed. Genes represented by more than one probe on the microarray were called differentially expressed if at least 50% of the probes fulfilled the cut-off requirements. Gene expression profile data was visualized and manipulated in Spotfire DecisionSite 6.3

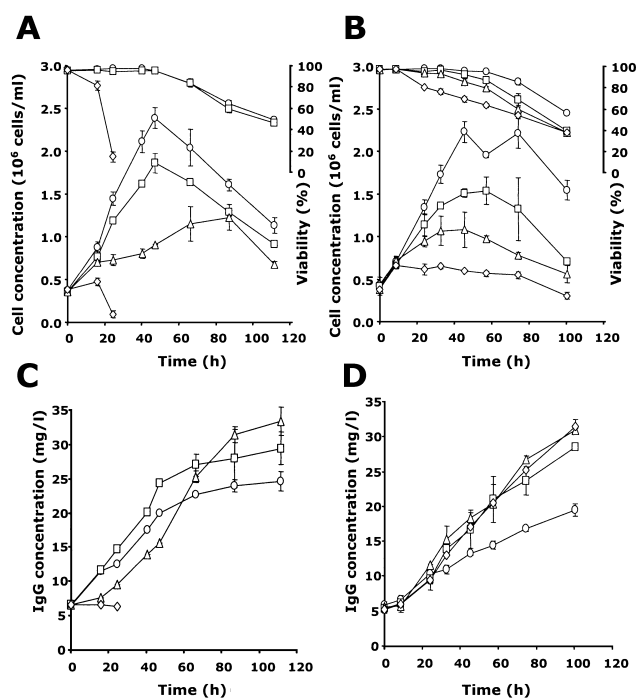


FIG. 1. Cell growth, viability and IgG concentration for sodium butyrate treated (A, B) mouse hybridoma and (C, D) CHO cell cultures. Sodium butyrate treatment concentrations: 0 mM (circles), 0.5 mM (squares), 1 mM (triangles), and 2 mM (diamonds). The 0 h microarray sample was taken at the time of butyrate addition.

(Spotfire, Somerville, MA, USA). Differentially expressed genes were clustered with gCluto (<http://www-users.cs.umn.edu/~karypis/cluto/gcluto/>).

RESULTS

Effect of butyrate on cell growth and cell productivity

The effects of butyrate on cell growth and antibody production were examined at three concentrations (0.5, 1, and 2 mM) using exponentially growing CHO and mouse hybridoma cells. Cultures without butyrate were used as a control. The effect of butyrate can be seen by the progressively reduced growth rate and maximum growth extent with increasing butyrate concentration (Fig. 1). For mouse hybridoma cells treated with 2 mM sodium butyrate, cell growth and IgG production stopped almost immediately. Only 24 h after butyrate addition, the viability had dropped to 20%. Treatment with both 0.5 and 1 mM butyrate slowed growth, and increased total IgG production as compared to the untreated control cells, without the drastic reduction in viability observed at the 2 mM concentration.

The response of CHO cells to butyrate addition was simi-

lar to that observed in mouse hybridoma cells. Peak cell concentration progressively decreased with increasing butyrate concentration. Cell growth in the 2 mM sodium butyrate treated culture essentially stopped 10 h after butyrate addition, but a rapid decline in viability was not observed for CHO cells, as compared with the response of hybridoma cells treated with 2 mM sodium butyrate. The IgG concentration for all butyrate-treated CHO cultures was higher than the untreated culture.

In both mouse hybridoma and CHO cells, 2 mM butyrate treatment elicited the most dramatic effect on cell growth; however, the severe decrease in viability observed for hybridoma cells at 2 mM butyrate concentration prompted us to choose treatment with 1 mM sodium butyrate for the comparative transcription profiling studies.

Dynamics of differentially expressed transcripts

CHO and hybridoma cells were inoculated in spinner flasks and grown for 24 h. At this time, the cells were treated with sodium butyrate (1 mM) and transferred into T-75 flasks, which were subsequently harvested for RNA extraction at 2, 4, 8 and 27 h after butyrate addition. A 0 h sample (at the time of butyrate addition) was used as the reference hybridization sample for comparison of each time point. Hybridoma cell RNA samples were hybridized to BMAP microarrays, and CHO cell RNA samples were hybridized to both BMAP and CHO microarrays. Four hybridizations were performed at each time point as duplicate dye-swaps.

Despite the seemingly profound physiological response observed in cells treated with sodium butyrate, the vast majority of transcripts did not exhibit significant dynamic behavior over the 27 h period. Among the genes that were determined to have a changing expression pattern, the magnitude of change typically increased progressively over the time course, and exhibited the highest degree of altered expression at the 27 h time point. Table 1 summarizes the number of genes observed to be changing in the hybridoma and CHO cell time profiles. Overall, the number of genes changing expression is higher in mouse hybridoma cells than in CHO cells as determined by the hybridoma:BMAP and CHO:CHO microarray hybridizations. The smaller number of probes on the CHO microarray certainly contributes to this difference; however, even the percentage of unique transcripts changing was greater in mouse hybridoma cells (13.7% in MAK vs. 4.1% in CHO). When the gene representation is expanded for CHO cells by using the mouse BMAP microarray by cross-species hybridization, only 4.5% of probes were identified as differentially expressed. Even though a lower number of genes were identified as differentially expressed in the CHO:BMAP hybridization as well as the CHO:CHO microarray, caution should be extended in the interpretation of these results. The number of genes classified as differentially expressed by the cross-species hy-

TABLE 1. Summary of the number of significantly differentially expressed transcripts for CHO cells and hybridoma cells exposed to 1 mM sodium butyrate using both mouse BMAP and CHO cell DNA microarrays

Cell	Total number of non-redundant genes on the array	Number of non-redundant genes differentially expressed	Percentage of non-redundant genes differentially expressed (%)
CHO:CHO	2602	122	4.7
CHO:mouse	6608	295	4.5
Hybridoma:mouse	6608	916	13.9

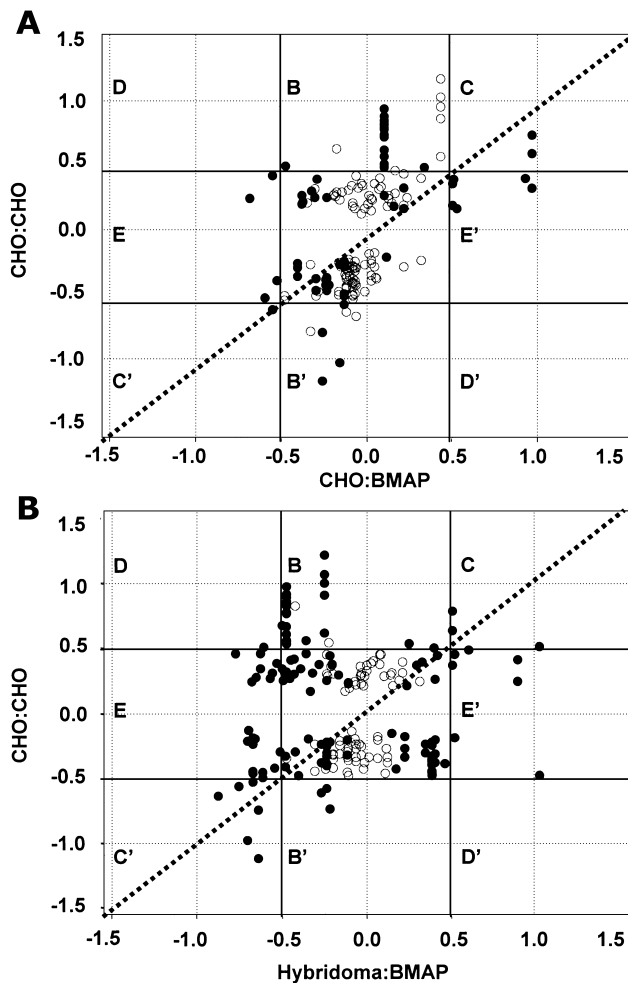


FIG. 2. Comparison of \log_2 of intensity ratios for 143 orthologous genes from CHO and BMAP microarrays. (A) Comparison of CHO:CHO (same species) hybridization with CHO:BMAP (cross-species) hybridization. (B) Comparison of CHO:CHO hybridization with hybridoma:BMAP hybridization. All spots of orthologous genes shown have a p -value ≤ 0.05 in the CHO:CHO hybridization. Dark circles are those with p -value ≤ 0.05 , open circles have a p -value > 0.05 in the CHO:BMAP (A) or hybridoma:BMAP (B) hybridizations.

bridization could be affected by the lower sequence homology between the mouse probes and CHO cell transcripts.

Through BLAST comparison, 143 EST sequences present on both CHO and mouse BMAP microarrays were identified as orthologous with a high level of confidence (BLAST score > 300). In mouse hybridoma cells, 32 of these orthologous genes were differentially expressed. In CHO cells, 21 genes within the set were differentially expressed in both the CHO:CHO microarray hybridization and the cross-species hybridization (CHO:BMAP). The expression levels of this orthologous set are compared and shown in Fig. 2.

To assess the agreement between the CHO:CHO and CHO:BMAP hybridizations, the transcript level changes for all orthologous genes present on both the CHO and BMAP microarrays were compared at the 27 h time point. The \log_2 of the ratio of all of the orthologous sequences which exhibit a p -value < 0.05 in the CHO:CHO hybridization dataset are plotted against that of each corresponding mouse se-

quence on BMAP microarray (Fig. 2A). The data from the CHO:BMAP hybridization are further divided into two categories: those with a p -value < 0.05 (Fig. 2A, dark circles), and those with a p -value > 0.05 (Fig. 2A, open circles). Bold vertical and horizontal lines are drawn at the -0.5 and 0.5 \log_2 ratio to show the approximate bounds of the 1.4-fold expression change cutoff that we used for calling differential expression in this work. Spots enclosed in the center square are not considered differentially expressed, even though their p -value in the CHO:CHO hybridization is less than 0.05. The orthologous genes which are not included in this plot generally have a \log_2 expression ratio near zero and, consequently, have a larger p -value. For some genes, more than one probe is present on a microarray; therefore, a single gene may be represented by more than one marker. Spots lying in the regions labeled C and C' (outside of the 0.5 to 0.5 square) are those with a greater than 1.4-fold change in the same direction in both CHO:CHO and CHO:BMAP hybridizations. These transcripts are differentially expressed consistently in both same-species and cross-species hybridizations. Those falling in the regions D or D' were called differentially expressed in opposing directions by the two hybridizations. Few data points fall into the areas labeled D or D' indicating the two hybridizations did not give rise to contradicting results. Overall, the data align with the diagonal dashed line shown, suggesting a general agreement between the two hybridizations. While the data are largely in agreement, a significant number of markers are open circles (p -value > 0.05) and would not have been identified as differentially expressed in the cross-species hybridization data.

The transcript data of orthologous genes for CHO and MAK cells obtained from their respective same species hybridization were similarly plotted to compare their response to butyrate treatment (Fig. 2B). No data points are present in the D or D' regions; thus, none of the orthologous genes are differentially expressed in opposite directions in response to butyrate treatment. Overall, the number of genes changing expression and the extent of those changes are relatively small, but the trend of all data points lies along the dashed diagonal line in Fig. 2B, suggesting that there is agreement between the response of CHO and MAK cells to butyrate treatment. The genes differentially expressed similarly in both CHO and hybridoma cells (lie in regions C and C') are listed in Table 2. Additionally, several genes were called differentially expressed in only one of the cell lines, but not in the other. These genes are represented by the spots in regions B, B', E, and E'. For many of these genes, the transcript levels had an agreeing trend with statistically significant p -values in both cell lines (p -value < 0.05 , dark circles). However, these genes were not called differentially expressed because the fold-change is less than 1.4. The identities of these genes are also included in Table 2.

Differential expression of physiologically relevant transcripts Because of the lower degree of confidence in the results of the CHO:BMAP hybridization, in the following sections we will focus on data from the CHO:CHO and MAK:BMAP hybridizations. The differentially expressed genes identified at each time point were grouped into a number of relevant gene classes based on gene ontology. Figure 3 shows the number of differentially expressed genes

TABLE 2. Summary of genes consistently up-regulated and down-regulated in CHO and hybridoma cells upon treatment with 1 mM sodium butyrate

Gene description	CHO cells (CHO array)		CHO cells (BMAP array)		Hybridoma cells (BMAP array)		% identity CHO/ mouse seq
	Fold change	<i>p</i> -value	Fold change	<i>p</i> -value	Fold change	<i>p</i> -value	
Up-regulated in butyrate treated culture							
Statistically significant in both CHO and hybridoma cells							
Cytochrome <i>c</i> oxidase subunit VIIa 2/3	+1.4	4.1E-07	+1.2	1.8E-01	+1.5	9.0E-06	89.4
Vimentin	+2.0	2.0E-08	–	–	+1.4	5.9E-08	87.0
Thymosin, beta 4, X chromosome ^a	+1.6	4.9E-08	+2.0	1.3E-12	+1.4	1.2E-02	95.0
Statistically significant in one cell line (agreeing trend in the other)							
ADP-ribosylation factor-like 6 interacting protein 1	+1.2	6.8E-02	+1.3	1.4E-01	+1.4	4.8E-06	87.0
RIKEN cDNA 231005K10 gene (hypothetical polyadenylate binding protein-interacting protein 2) ^a	+1.2	8.3E-02	+1.2	2.3E-02	+1.4	2.0E-08	89.6
Thymosin, beta 10 ^a	+1.3	1.9E-07	+1.4	8.6E-06	+1.8	5.8E-07	93.8
Aldo-keto reductase family 1, member B3 (aldose reductase) ^a	+1.4	1.9E-06	+1.3	3.9E-03	+1.2	3.1E-05	95.0
RIKEN cDNA 2410005K17 gene	+1.4	6.7E-06	+1.1	4.3E-01	+1.3	3.3E-06	85.0
Mus musculus similar to NADH-ubiquinone oxidoreductase B17 subunit (Complex I-B17), mRNA	+1.4	8.1E-10	+1.1	2.3E-01	+1.3	5.9E-03	87.0
Down-regulated in butyrate treated culture							
Statistically significant in both CHO and hybridoma cells							
Mortality factor 4 like 2 ^a	–1.5	9.6E-06	–1.5	3.0E-03	–1.7	3.6E-07	97.7
Nucleophosmin 1 ^a	–1.7	2.7E-06	–1.2	2.7E-02	–1.6	7.8E-09	95.0
Peptidylprolyl isomerase A (cyclophilin) ^a	–1.4	1.3E-04	–1.1	4.5E-02	–1.6	6.5E-12	91.0
Proteasome (prosome, macropain) subunit, alpha type 4	–1.6	4.6E-06	–	–	–1.8	5.8E-07	90.0
RAS-like, family 2, locus 9	–1.6	2.1E-06	–	–	–2.5	5.0E-04	88.0
RIKEN cDNA 2410005K20 (hypothetical ribosomal protein L1) ^a	–1.5	1.2E-06	–1.5	6.2E-04	–2.1	3.9E-12	97.0
Proteasome (prosome, macropain) 26S subunit, ATPase, 6	–1.4	2.6E-08	–1.4	1.7E-01	–1.5	2.6E-02	90.0
Solute carrier family 25 (mitochondrial carrier; adenine nucleotide translocator), member 5 ^a	–2.0	2.2E-10	–1.1	1.6E-03	–1.6	3.2E-13	94.0
Thioredoxin 1	–1.5	1.1E-04	–1.0	3.6E-01	–1.4	2.2E-10	90.0
Statistically significant in one cell line (agreeing trend in the other)							
ATPase, Na ⁺ /K ⁺ transporting, beta 3 polypeptide	–1.3	8.8E-06	–1.2	1.2E-01	–1.5	5.9E-05	90.0
H2A histone family, member Z ^a	–1.3	6.9E-03	–1.3	1.1E-03	–1.7	1.9E-12	92.0
Heterogeneous nuclear ribonucleoprotein A2/B1 ^a	–1.2	4.7E-01	–1.6	1.6E-05	–2.4	7.7E-09	91.0
Karyopherin (importin) beta 1 ^a	–1.1	1.4E-01	–1.5	1.3E-05	–2.4	1.8E-18	94.0
Eukaryotic translation elongation factor 1 beta 2 ^a	–1.7	1.5E-06	–1.3	6.1E-02	–1.2	2.9E-02	91.2
Ribosomal protein S3a or 40S ^a	–1.5	1.5E-07	–1.1	5.3E-02	–1.2	1.4E-07	91.0
Bleomycin hydrolase ^a	–1.4	3.9E-07	–1.5	6.1E-05	–1.3	2.3E-03	88.0
Acidic nuclear phosphoprotein 32 family, member B	–1.6	2.8E-03	–	–	–1.4	1.1E-04	98.0
Heterogeneous nuclear ribonucleoprotein D	–1.6	2.8E-08	–	–	–1.1	1.0E-02	91.0
Signal sequence receptor, alpha	–1.4	1.2E-08	–	–	–1.2	2.3E-02	88.0
Serine/threonine kinase receptor associated protein	–1.5	1.6E-03	–1.0	9.7E-01	–1.1	5.6E-02	87.0

Differentially expressed transcripts with a high statistical confidence (>1.4-fold expression change, <0.05 *p*-value) in both cell lines, or with statistical confidence in one of the cell lines, but showing agreement in expression in the other cell line are shown. Fold change (treated/untreated) and *p*-values for the 27 h time point are shown for each cell line/microarray combination. Percent identity for the mouse and CHO probe sequence alignments are also shown.

^a Genes those having a *p*-value<0.05 in the CHO:BMAP hybridization.

in each class for the entire time profile using the MAK:BMAP and CHO:CHO hybridization data. For mouse hybridoma cells (Fig. 3A), genes involved in cholesterol metabolism, cell cycle/growth, apoptosis, and histone modification responded quickly to butyrate treatment. Some of the genes within these classes have been identified previously as having butyrate-responsive promoters, notably HMG-CoA synthase 1 (10). As time advances, genes in these classes remain differentially expressed throughout the time profile. At later time points, genes from other important classes, including nucleotide metabolism, translation regulation, chaperones, and oxidative stress response, become differentially expressed. Coordinately with these gene changes, a de-

creased growth rate and increased IgG production rate was observed in the hybridoma culture.

In CHO cells (Fig. 3B), genes involved in apoptosis and protein folding (chaperones), are differentially expressed early following butyrate treatment. The response of apoptosis genes is similar to that seen in the hybridoma culture, while the response of chaperones was slightly more delayed (differentially expressed at the 8 h time point) in hybridoma cells. Due to the smaller number of gene probes and differing gene representation on the CHO microarray, one cannot definitively determine if there is an absence of an early response in other classes like cholesterol metabolism or cell cycle. Examination of the cross-species hybridization data

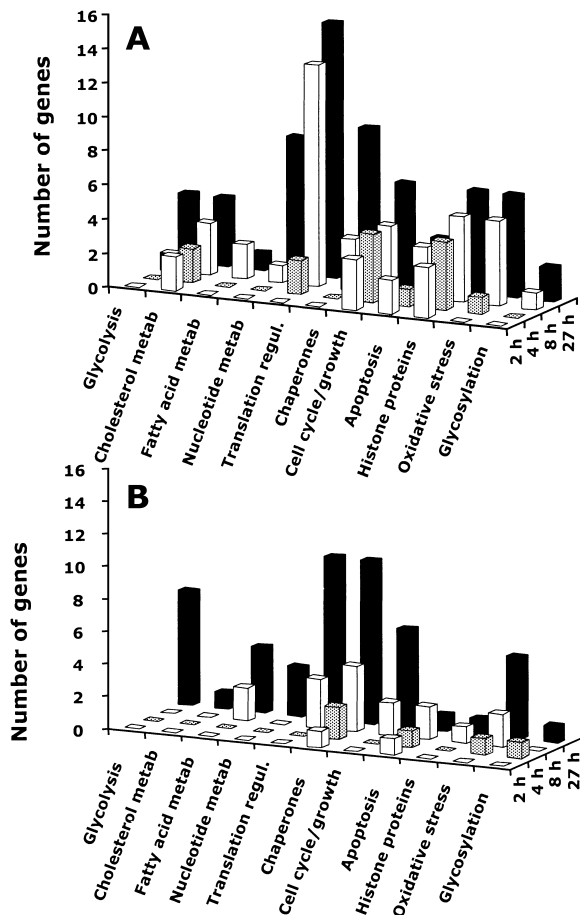


FIG. 3. Time profile of differential expression in important ontological classes following 1 mM sodium butyrate treatment for (A) Hybridoma:BMAP and (B) CHO:CHO microarrays. Differential expression is determined as p -value < 0.05, fold-change > 1.4.

for CHO cells similarly shows no alteration in the dynamics of gene expression for these classes; however, because fewer genes were identified as differentially expressed within this dataset, this absence could be a result of the lower sensitivity in detecting differential expression in the cross-species dataset. Eventually, genes involved in cell cycle/growth become more prominently affected in CHO cells at the 8 h time point. Genes from other classes, including glycolysis, fatty acid metabolism, nucleotide metabolism, translation regulation, chaperones, and oxidative stress response were also observed to be significantly changed in CHO cells, similar to the changes observed in hybridoma cells at the later time points.

Overall, the changes in differentially expressed genes appear to be in agreement with the observed physiological changes in cell growth, viability, and other known effects of butyrate treatment. One of the first responses observed in both CHO and hybridoma cells after butyrate treatment is alteration of apoptosis related genes. Butyrate is cytotoxic, thus the response in apoptosis genes and oxidative stress genes is not unexpected. Additionally, in the later time points an alteration in metabolism is observed in both cells. Among the glycolysis genes present on the two arrays, very few are present on both microarrays, except for lactate de-

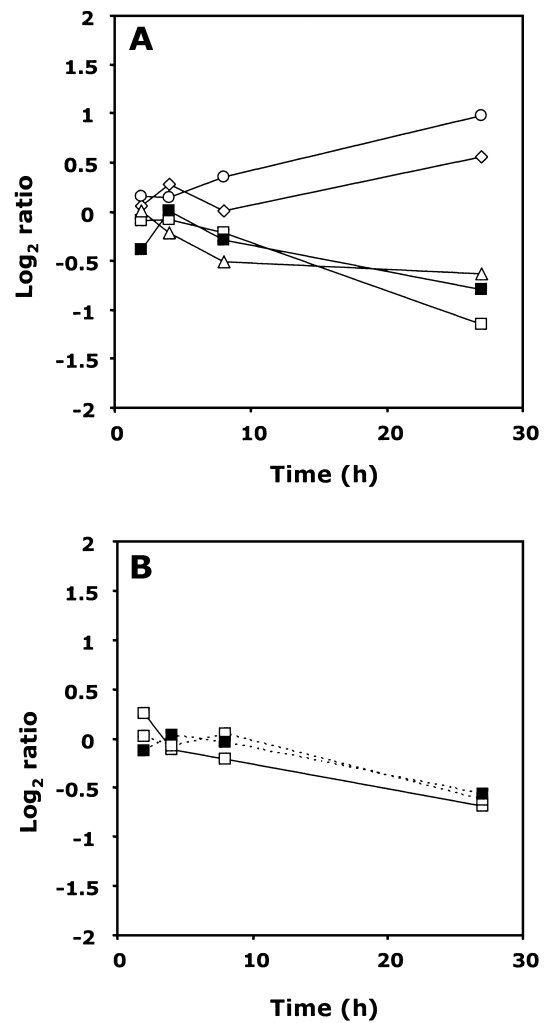


FIG. 4. \log_2 intensity ratio time profile for differentially expressed glycolysis genes for hybridoma cells (A) and CHO cells (B). Data from the mouse BMAP microarray: lactate dehydrogenase 1, A chain (open squares); lactate dehydrogenase 2, B chain (dark squares); glyceraldehyde-3-phosphate dehydrogenase (open diamonds); aldolase 3, C isoform (open circles); phosphoglycerate mutase 1 (open triangles). Data from the CHO cell array: lactate dehydrogenase (open squares). Data points obtained from the CHO microarray are connected by dark solid lines. Data from the cross species (CHO:BMAP) hybridization are connected by dashed lines.

hydrogenase (LDH). Time profiles of the \log_2 ratios for differentially expressed glycolysis genes for hybridoma cells and CHO cells are shown in Fig. 4A and 4B, respectively. Both cell lines show a down-regulation in all measured isoforms of LDH. This trend was also observed in the cross-species hybridization results. With the decreased growth rate observed in both cell lines, an alteration in metabolism is expected; however, the nature of these changes cannot be discerned with the limited probes available for this pathway, especially in CHO cells. In hybridoma cells, three other well-known glycolysis genes changed over time. Phosphoglycerate mutase 1 (PGM1) showed a similar decreasing trend as LDH, while aldolase and glyceraldehyde 3-phosphate dehydrogenase were both up-regulated at later time points.

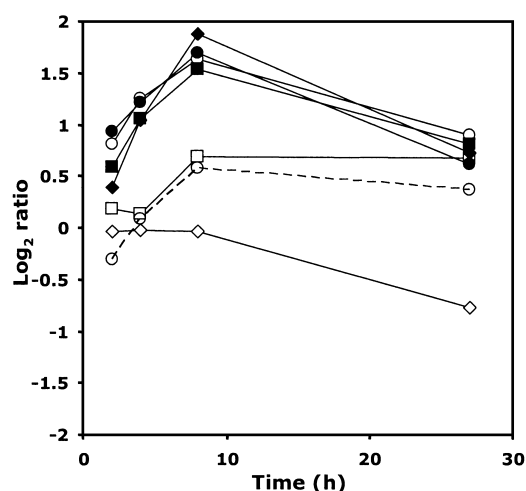


FIG. 5. Log_2 intensity ratio time profile for differentially expressed histone proteins. Same species hybridization data (Hybridoma: BMAP and CHO: CHO) are drawn with thin solid lines. CHO: BMAP data are drawn with dashed lines. Histone proteins plotted include H1 member 0 (open circles), H1a (dark circles), H2A member V (open squares), H2a member X (dark squares), H2a member z (open diamonds) and H2bc (dark diamonds).

Histone and chromatin structure related genes were also among those with a higher degree of differential expression, showing an early response upon butyrate treatment in hybridoma cells, and a later response in those genes available on the CHO microarray. The time profiles of the log_2 ratios for histone and chromatin structure related genes are shown in Fig. 5. In mouse hybridoma cells, histone 1 proteins were up-regulated progressively in the first few hours after butyrate addition, but subside in their expression level at the 27 h time point. Such drastic up-regulation shortly after butyrate addition has been reported previously (11, 12). Histone 1 is a linker protein that maintains a condensed nucleosome structure. Additionally, sodium butyrate is known to have deacetylation inhibitor activity, which would induce a relaxation in nucleosome structure. It is thought that cells respond to the nucleosome decondensation by up-regulating histone 1 proteins, which function as nucleosome linkers.

Additionally, a correlation has been identified between histone H1(0) gene expression and histone acetylation by treatment with a similar agent (13). Trichostatin (TSA), another histone deacetylase inhibitor, has also been shown to efficiently induce histone H1(0) expression. Interestingly, in this study, it was found that not only histone 1 proteins but also genes from histone 2A and 2B families were differentially expressed. For CHO cells, an up-regulation of H1(0) was also observed, although to a lesser extent. Little overlap exists among these specific genes between the two microarrays; yet the data clearly confirms the role of sodium butyrate in the alteration of chromatin structure.

Changes in cholesterol and fatty acid metabolism genes were also observed upon sodium butyrate treatment. The response was more pronounced in mouse hybridoma cells, although the limited availability of relevant probes on the CHO microarray warrants further investigation of a similar response in CHO cells. Time profile data for cholesterol metabolism genes revealed that the enzyme 3-hydroxy-3-meth-

ylglutaryl-Coenzyme A synthase 1 (HMG-CoA synthase 1) was slightly up-regulated in early time points (at 4 h, $\text{log}_2=0.45$, $p\text{-value}=5.11 \times 10^{-5}$), then decreased its expression to the point where it is significantly down-regulated at the end of the culture (at 27 h, $\text{log}_2=-0.88$, $p\text{-value}=2.22 \times 10^{-10}$). While this probe was not available on the CHO cDNA microarray, the cross species hybridization data showed down-regulation of its transcript level in CHO cells at the 27 h time point (at 27 h, $\text{log}_2=-0.54$, $p\text{-value}=4.18 \times 10^{-8}$). HMG-CoA synthase 1 is a cytosolic enzyme, and functions to condense acetyl CoA to form HMG-CoA, which then enters endoplasmic reticulum and peroxisome for isoprenoid and cholesterol biosynthesis. HMG-CoA synthase 1 is known to be induced by butyrate treatment (10). Additionally, the expression of HMG-CoA synthase 1 is regulated by sterol regulatory element binding proteins (SREBP) (14). In the hybridoma cell expression results, one of the sterol regulatory element binding proteins, SREBP1, was found to increase after butyrate addition, reaching its highest expression at the 8 h time point (at 8 h, $\text{log}_2=0.67$, $p\text{-value}=1.30 \times 10^{-5}$). Farnesyl diphosphate synthetase, another enzyme regulated by SREBP1 had a similar expression profile as SREBP1 (at 4 h, $\text{log}_2=0.51$, $p\text{-value}=1.11 \times 10^{-2}$). An increased transcription level of SREBP1 and its corresponding response genes suggests an up-regulation of fatty acid synthesis, which is in agreement with the observed changes in fatty acid metabolism in both CHO and MAK cells.

Sodium butyrate has been reported to impair lipid transport (15). In these microarray experiments, the very low-density lipoprotein (VLDL) receptor was down-regulated at the later time points (at 27 h, $\text{log}_2=-0.73$, $p\text{-value}=6.90 \times 10^{-8}$). There is evidence that SREBP may also regulate the VLDL assembly/secretion pathway (16). The combination of these microarray results provides more evidence of significant interplay between the regulatory protein SREBP and its potential targets.

Sterol O-acyltransferase 1, which plays a role in lipoprotein assembly by catalyzing the formation of fatty acid-cholesterol esters, showed a steadily increasing up-regulated time profile (at 27 h, $\text{log}_2=1.41$, $p\text{-value}=2.50 \times 10^{-12}$). The expression of cellular nucleic acid binding protein (CNBP), also involved in the production of low density lipoprotein (LDL) (17), was also affected, showing a sharply down-regulated trend (at 27 h, $\text{log}_2=-1.22$, $p\text{-value}=1.47 \times 10^{-2}$). The LDL receptor-related protein 1 was also down-regulated in hybridoma cells, indicating a potential decrease cholesterol uptake. As a whole, there was an observed trend of decreasing availability of cholesterol in hybridoma cells following sodium butyrate treatment. The response of these genes in CHO cells are not known, due to their absence on the CHO microarray. Those probes present on the BMAP microarray did not show significant expression changes in the cross-species data. Even without clear evidence of alteration of lipid metabolism in the CHO cell data, the significance of the changes observed in hybridoma cells warrants further investigation in CHO cells, and other recombinant host cell lines.

As sodium butyrate is known to increase recombinant protein production, it was somewhat unexpected that the microarray results significantly indicated a global down-regula-

tion of mRNA translation and protein synthesis. Initiation of translation is the key controlling step in eukaryotic protein expression. Changes in the activity or abundance of translation initiation factors mediate a global change in translation rate. A significant down-regulation of translation initiation factors was seen in both mouse and CHO cells exposed to sodium butyrate. For CHO cells, a down-regulation of eukaryotic translation initiation factors 5 and 5A was observed on both the CHO:CHO (at 27 h, 5: $\log_2 = -0.37$, p -value = 1.00×10^{-2} , 5A: $\log_2 = -0.87$, p -value = 2.55×10^{-13}) and CHO:BMAP hybridizations (at 27 h, 5: $\log_2 = -0.97$, p -value = 1.96×10^{-7} , 5A: $\log_2 = -0.66$, p -value = 2.55×10^{-3}). Other genes known to be involved in translation initiation were down-regulated, including four genes involved in tRNA aminoacylation, and tRNA ligase activity for aspartate, glutamine, glycine and threonine.

A number of chaperones and heat shock proteins were also differentially expressed in both hybridoma and CHO cells. In hybridoma cells, chaperonins and heat shock proteins, were generally down-regulated. This coincides with the observed decrease in protein translation machinery. Another class of chaperones, the glucose regulated proteins (GRPs), were up-regulated in both hybridoma and CHO cells after sodium butyrate treatment. In the hybridoma culture, GRP94 was slightly up-regulated (at 27 h, $\log_2 = 0.52$, p -value = 2.60×10^{-6}), and the CHO cell GRP78 (also known as BiP) was highly up-regulated, with a 2-fold increase in expression level at the 27 h time point. GRP78 is not included on the BMAP microarray, so the response of the hybridoma ortholog is unknown. GRP78 and GRP94 are both localized in the endoplasmic reticulum (ER). Their expression is induced in response to various stress conditions, and they share a common regulatory element in their promoter region (18). Their increased expression level is possibly related to the stress induced by sodium butyrate addition.

DISCUSSION

Large-scale transcript profiling using DNA microarray has proven a powerful tool for in biological research; however, their application in industrial bioprocessing, specifically in mammalian cell culture based processes, is still relatively limited. It is likely that the limited availability of sequence information and DNA microarrays for CHO cells has hampered efforts on transcriptome analysis. With complete genomic resources and many tools widely available for mouse, it is attractive to explore the utility of mouse sequence based microarrays in the study of CHO cells. Cross-species hybridization has been used previously to study gene expression in species with similarly little resources. For example, human arrays have employed in transcriptome analysis of pigs (19, 20). Relatively consistent results were obtained between corresponding human and pig mRNA experiments; however, it was noted that several probes had no detectable signal and were excluded from the analysis. In that study, hybridization conditions were optimized for highly stringent sequence specificity, increasing the likelihood that genes with less sequence homology were excluded in the analysis.

Such variation in the extent of homology among ortholo-

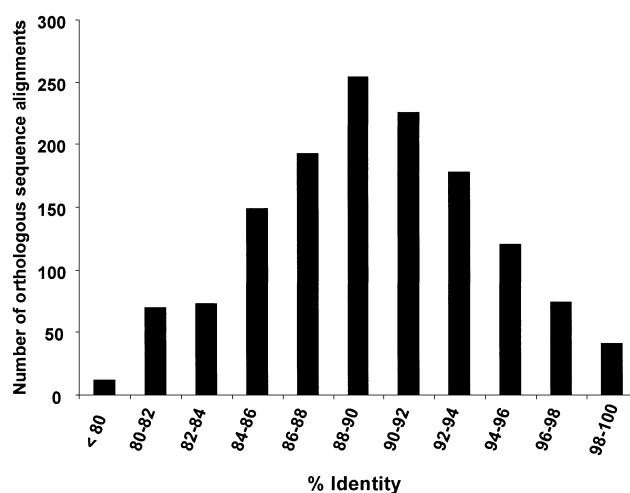


FIG. 6. Frequency distribution of base pair % identities among 100 or longer aligning segments of CHO microarray and mouse BMAP microarray probe sequences.

gous gene pairs between two species affects each probe's reliability in detecting changes in transcript levels in cross species hybridization. Through EST sequencing of CHO cell cDNA libraries, the sequence percent identity between orthologous genes of CHO and mouse was determined to range between 70%–97% (7). To assess the variability in homology among the orthologous genes used in this study, the BLAST alignment of CHO probe sequences with BMAP probe sequences was further examined. Between the CHO and BMAP microarrays, 1393 probe pairs were identified as having an aligning segment of greater than 100 base pairs. The percent identities for those 1393 sequence pairs were calculated and plotted as a frequency distribution (Fig. 6). The percent identity ranged from 80% to 100% among the aligning segments, however its range spans from 80% to 99.5%. To assess the relationship between percent identity and the agreement between same species and cross species hybridization, the orthologous CHO and BMAP probes which gave rise to consistent differential expression calls were further analyzed. Table 2 lists the microarray analysis results and the percent identity between the CHO and BMAP probe sequences. Within this set of genes with agreeing expression trends, those for which the cross-species hybridization data yielded a small p -value (<0.05) are highlighted. It can be seen that the percent identities for the CHO and mouse probe alignments for these highlighted probes are generally above 89–90%. Conversely, the percent identities in the non-highlighted rows, where the cross-species hybridization gave less reliable results (p -values >0.05), are below 90%.

The results in Table 2 suggest that probes with an 89–90% identity or greater will give rise to reliable differential expression calls, even in the cross species hybridization. However, the identity frequency distribution data shown in Fig. 6 indicate that only about half of the orthologous probes would have an identity greater than 89%. With only half of the probes providing potentially reliable results, much of the hybridization data will still be clouded with uncertainty.

The range of sequence identity between mouse and

Chinese hamster is similar to the range of identity between pig and human (19, 21). A lower signal intensity and decreased statistical confidence was reported in the pig:human cross-species hybridizations, similar to our results obtained from the CHO:BMAP hybridizations. Conversely for human and primate, for which the degree of homology is high (98% between humans and chimpanzees) (22), the use of cross-species hybridization for primate mRNA to human microarrays is more likely to give reliable results (23). Undoubtedly, even for highly similar species like primate and human, same species hybridization is a preferred approach for DNA microarray experiments. Even with the high level of similarity between humans and primates, there is an extensive effort for development of genomic tools and resources for Chimpanzee, Rhesus Monkey, Orangutan, and Gibbon by the NIH National Human Genome Research Institute (<http://www.genome.gov/10002154>). Unfortunately, efforts to sequence a sufficient number of ESTs or an entire mammalian genome is still costly, and is not likely to be realized for hamster species in the near future.

We took a comparative transcript profiling approach by examining gene expression of antibody producing cells from two species: a recombinant antibody producing CHO cell line, and a mouse hybridoma cell line, both treated with sodium butyrate during exponential growth phase. In this study, both the species and cell lineage differ (one from lymphatic system, the other from a reproductive organ), but the response of increased productivity using treatment with butyrate is known to be similar, and is expected to elicit profound and conserved changes in gene expression. The combination of the mRNA samples and the two DNA microarrays used allow us to compare the transcriptional response of two cell lines to exposure to butyrate, and, at the same time, evaluate the effectiveness of the use of mouse microarrays for cross-species hybridization of CHO mRNA.

It was expected that the cross-species hybridization (CHO:BMAP) would serve to supplement the probes available for physiological interpretation in CHO cells; however, the cross-species hybridization results did not substantially increase the number of differently expressed genes identified. The lack of statistical confidence level in the results obtained by cross-species hybridization made identifying true differential expression difficult. It is plausible that further optimization of hybridization conditions (*e.g.*, increasing the hybridization temperature) or examination of the level of conservation between orthologous sequences could yield a more reliable cross-species hybridization dataset; however, there will always be lingering uncertainty about the reliability of the data generated in the absence of more CHO sequence information. Overall, a higher percentage of mouse genes were differentially expressed as compared to CHO genes. This may reflect the increased sensitivity of hybridoma cells to butyrate treatment at the concentration used in this study. The maximum affect on antibody production was seen at 1 mM for hybridoma cells, but for CHO cells, a more profound affect was seen at a higher concentration (2 mM). Additionally, the fewer number of changed genes in the CHO cell experiment could be a result of the decreased gene coverage on the CHO array, and the reduced statistical confidence in identifying differentially expressed

genes using cross-species hybridization.

Most gene expression changes are observed at the later time points (8 and 27 h). The response of the gene classes after 27 h is similar in both cell lines. Many results confirm known effects of sodium butyrate treatment. Histone acetylation destabilizes chromatin structure and facilitates transcription (21, 24–27). In previous work, genes were observed to respond to butyrate treatment, however it was not well understood why those genes were affected. One hypothesis is that promoter of the changed gene could be susceptible to the effects of sodium butyrate (10). Another hypothesis is that the transcription factors controlling the expression of those genes are susceptible to the acetylation/deacetylation affects of butyrate (28).

It is not clear why the addition of sodium butyrate leads to increased production of recombinant proteins in cultured mammalian cells. The enhancing effect of heterologous genes was seen across product genes under the control of different promoters, in a study of cytomegalovirus (CMV) (3, 29) and simian virus 40 (SV40) promoters respectively. In the sodium butyrate treated CHO cells, both DHFR and the recombinant product were significantly up-regulated according to the CHO:CHO microarray data. In contrast, transcripts for genes involved in translation and early protein folding appear to be down-regulated upon butyrate addition. The answer to this paradox awaits further study. Of course, one may argue that with the microarrays used in these studies, the gene coverage is still insufficient to reveal the true mechanism, particularly for the CHO microarray.

In view of the reduced level of confidence in the cross-species hybridization experiment, it appears necessary to further sequence CHO ESTs to develop a more comprehensive CHO microarray. In this study, we took a comparative transcriptome analysis approach comparing two cell lines treated with similar conditions. We observed more similarity than dissimilarity in the transcriptional response of CHO and mouse hybridoma cells, even considering that the two cell lines originate from very different species and tissue lineages. Although no obvious transcript changes lead to a definite mechanistic interpretation, the similarity in their transcript profiles was consistent with the enhanced productivity seen in both cell lines.

ACKNOWLEDGMENTS

MLG was supported by an NIH Biotechnology Training Grant (GM08347) and a University of Minnesota Graduate School fellowship. KFW was also supported by an NIH Biotechnology Training Grant (GM08347) and by a National Science Foundation fellowship. We thank the generous gift from Merck & Co.

REFERENCES

1. **Seth, G., Hossler, P., Yee, J. C., and Hu, W. S.:** Engineering cells for cell culture bioprocessing—physiological fundamentals. *Adv. Biochem. Eng. Biotechnol.*, **101**, 119–164 (2006).
2. **Sung, Y. H., Song, Y. J., Lim, S. W., Chung, J. Y., and Lee, G. M.:** Effect of sodium butyrate on the production, heterogeneity and biological activity of human thrombopoietin by recombinant Chinese hamster ovary cells. *J. Biotechnol.*, **112**, 323–335 (2004).

3. **Palermo, D. P., DeGraaf, M. E., Marotti, K. R., Rehberg, E., and Post, L. E.:** Production of analytical quantities of recombinant proteins in Chinese hamster ovary cells using sodium butyrate to elevate gene expression. *J. Biotechnol.*, **19**, 35–47 (1991).
4. **Oh, S. K. W., Vig, P., Chua, F., Teo, W. K., and Yap, M. G. S.:** Substantial overproduction of antibodies by applying osmotic pressure and sodium butyrate. *Biotechnol. Bioeng.*, **42**, 601–610 (1993).
5. **Mimura, Y., Lund, J., Church, S., Dong, S., Li, J., Goodall, M., and Jefferis, R.:** Butyrate increases production of human chimeric IgG in CHO-K1 cells whilst maintaining function and glycoform profile. *J. Immunol. Methods*, **247**, 205–216 (2001).
6. **Zhou, W. C., Rehm, J., and Hu, W. S.:** High viable cell concentration fed-batch cultures of hybridoma cells through on-line nutrient feeding. *Biotechnol. Bioeng.*, **46**, 579–587 (1995).
7. **Wlaschin, K., Nissom, P. M., de Leon Gatti, M., Fern, P. F. O., Arleen, S., Tan, K. S., Rink, A., Cham, B., Wong, K., Yap, M., and Hu, W. S.:** EST sequencing for gene discovery in Chinese hamster ovary cells. *Biotechnol. Bioeng.*, **91**, 592–606 (2005).
8. **Korke, R., de Leon Gatti, M., Lau, A. L., Lim, J. W., Seow, T. K., Chung, M. C., and Hu, W. S.:** Large scale gene expression profiling of metabolic shift of mammalian cells in culture. *J. Biotechnol.*, **107**, 1–17 (2004).
9. **Yang, Y. H., Dudoit, S., Luu, P., and Speed, T. P.:** Normalization for cDNA microarray data, p. 141–152. *In* Bittner, M. L., Chen, Y., Dorsel, A. N., and Dougherty, E. R. (ed.), *Microarrays: optical technologies and informatics*. Proceedings of SPIE BiOS 2001, vol. 4266. The International Society for Optical Engineering, Bellingham (2001).
10. **Camarero, N., Nadal, A., Barrero, M. J., Haro, D., and Marrero, P. F.:** Histone deacetylase inhibitors stimulate mitochondrial HMG-CoA synthase gene expression via a promoter proximal Sp1 site. *Nucleic Acids Res.*, **31**, 1693–1703 (2003).
11. **D'Anna, J. A., Tobey, R. A., and Gurley, L. R.:** Concentration-dependent effects of sodium butyrate in Chinese hamster cells: cell-cycle progression, inner-histone acetylation, histone H1 dephosphorylation, and induction of an H1-like protein. *Biochemistry*, **19**, 2656–2671 (1980).
12. **D'Anna, J. A., Gurley, L. R., Becker, R. R., Barham, S. S., Tobey, R. A., and Walters, R. A.:** Amino acid analysis and cell cycle dependent phosphorylation of an H1-like, butyrate-enhanced protein (BEP; H1(0); IP25) from Chinese hamster cells. *Biochemistry*, **19**, 4331–4341 (1980).
13. **Girardot, V., Rabilloud, T., Yoshida, M., Beppu, T., Lawrence, J. J., and Khochbin, S.:** Relationship between core histone acetylation and histone H1(0) gene activity. *Eur. J. Biochem.*, **224**, 885–892 (1994).
14. **Sakakura, Y., Shimano, H., Sone, H., Takahashi, A., Inoue, N., Toyoshima, H., Suzuki, S., Yamada, N., and Inoue, K.:** Sterol regulatory element-binding proteins induce an entire pathway of cholesterol synthesis. *Biochem. Biophys. Res. Commun.*, **286**, 176–183 (2001).
15. **Marcil, V., Delvin, E., Garofalo, C., and Levy, E.:** Butyrate impairs lipid transport by inhibiting microsomal triglyceride transfer protein in Caco-2 cells. *J. Nutr.*, **133**, 2180–2183 (2003).
16. **Kang, S. and Davis, R. A.:** Cholesterol and hepatic lipoprotein assembly and secretion. *Biochim. Biophys. Acta*, **1529**, 223–230 (2000).
17. **Rajavashisth, T. B., Taylor, A. K., Andalibi, A., Svenson, K. L., and Lusic, A. J.:** Identification of a zinc finger protein that binds to the sterol regulatory element. *Science*, **245**, 640–643 (1989).
18. **Chang, S. C., Erwin, A. E., and Lee, A. S.:** Glucose-regulated protein (GRP94 and GRP78) genes share common regulatory domains and are coordinately regulated by common trans-acting factors. *Mol. Cell. Biol.*, **9**, 2153–2162 (1989).
19. **Moody, D. E., Zou, Z., and McIntyre, L.:** Cross-species hybridisation of pig RNA to human nylon microarrays. *BMC Genomics*, **3**, 27 (2002).
20. **Gladney, C. D., Bertani, G. R., Johnson, R. K., and Pomp, D.:** Evaluation of gene expression in pigs selected for enhanced reproduction using differential display PCR and human microarrays: I. Ovarian follicles. *J. Anim. Sci.*, **82**, 17–31 (2004).
21. **Weich, N. S., Farlow, D., Poisson, L., He, R., Kim, M., Carroll, J., Nielsch, U., Mahmud, N., Hoffman, R., and Gutierrez-Ramos, J. C.:** Differential gene expression in non-human primate bone marrow following irradiation and administration of carboplatin. *Blood*, **98**, 551a (2001).
22. **Gu, J. and Gu, X.:** Induced gene expression in human brain after the split from chimpanzee. *Trends Genet.*, **19**, 63–65 (2003).
23. **Wang, Z., Lewis, M. G., Nau, M. E., Arnold, A., and Vahey, M. T.:** Identification and utilization of inter-species conserved (ISC) probesets on Affymetrix human GeneChip platforms for the optimization of the assessment of expression patterns in non human primate (NHP) samples. *BMC Bioinformatics*, **5**, 165 (2004).
24. **Wang, X., Moore, S. C., Laszczak, M., and Ausio, J.:** Acetylation increases the alpha-helical content of the histone tails of the nucleosome. *J. Biol. Chem.*, **275**, 35013–35020 (2000).
25. **Tse, C., Sera, T., Wolffe, A. P., and Hansen, J. C.:** Disruption of higher-order folding by core histone acetylation dramatically enhances transcription of nucleosomal arrays by RNA polymerase III. *Mol. Cell. Biol.*, **18**, 4629–4638 (1998).
26. **Nightingale, K. P., Wellinger, R. E., Sogo, J. M., and Becker, P. B.:** Histone acetylation facilitates RNA polymerase II transcription of the *Drosophila* hsp26 gene in chromatin. *EMBO J.*, **17**, 2865–2876 (1998).
27. **Hansen, J. C., Tse, C., and Wolffe, A. P.:** Structure and function of the core histone N-termini: more than meets the eye. *Biochemistry*, **37**, 17637–17641 (1998).
28. **Izumi, H., Ohta, R., Nagatani, G., Ise, T., Nakayama, Y., Nomoto, M., and Kohno, K.:** p300/CBP-associated factor (P/CAF) interacts with nuclear respiratory factor-1 to regulate the UDP-N-acetyl-alpha-d-galactosamine: polypeptide N-acetylgalactosaminyltransferase-3 gene. *Biochem. J.*, **373**, 713–722 (2003).
29. **Laubach, V. E., Garvey, E. P., and Sherman, P. A.:** High-level expression of human inducible nitric oxide synthase in Chinese hamster ovary cells and characterization of the purified enzyme. *Biochem. Biophys. Res. Commun.*, **218**, 802–807 (1996).